Journal of
Water & Climate Change

IWA PUBLISHING

Journal of Water and Climate Change Vol 13 No 3, 1548 doi: 10.2166/wcc.2022.351

Comparison of hydrogeochemical characteristics of thermokarst lake water in the Qinghai–Tibet Plateau under active layer freeze–thaw conditions

Yahong Fang[a,b], Zejun Liu[a,b], Qiaofen Lyu[a,b], Haiyang Hu[a,b] and Wei Wang[a,b,*]

[a] School of Water and Environment, Chang'an University, Xi'an, 710054 Shaanxi, China
[b] Key Laboratory of Subsurface Hydrology and Ecological Effect in Arid Region of the Ministry of Education, Chang'an University, Xi'an 710054 Shaanxi, China
*Corresponding author. E-mail: wangweichd@chd.edu.cn

WW, 0000-0002-4371-5714

ABSTRACT

With the gradual increase of global temperature, thermokarst lakes are widely developed and become major environmental disasters in the Tundra Plateau which have impacted the stability of the project such as the Qinghai–Tibetan highway. In this study, some typical thermokarst lakes in the Qinghai–Tibet Plateau (QTP) were selected as the research object. And four samples were taken from different freezing–thawing processes of the lakes in 2019 to analyze the hydrogeochemical process of the thermokarst lake in the context of climate change. Results show that the main hydrogeochemical types of the lake water in the northern part of the study area were HCO_3·Cl – Na·Ca·Mg or Cl·HCO_3 – Na·Mg, whereas in the central and southern parts were mainly Cl – Na·Mg. The variations of hydrogeochemical concentration in thermokarst lake water are mainly affected by evaporation concentration, rock differentiation, freezing desalination in the active layer, and plant photosynthesis, which are mainly due to temperature changes. Furthermore, the results of the saturation index (SI) show that dolomite and calcite leaching control the hydrogeochemical composition in thermokarst lakes. In addition, the evaporation-to-inflow (E/I) ratios of the lake reach the maximum in the middle and later periods of the active layer thawing. On the contrary, the E/I values of the lakes decrease during the initial thawing or freezing periods of the active layer.

Key words: climate change, hydrogeochemical processes, isotopes composition, Thermokarst lakes

HIGHLIGHTS

- First, the formation process of hot melt lakes in high-altitude areas is analyzed.
- Second, the chemical properties of the thermal melting lake in different regions are analyzed, and the reasons that affect the chemical properties are analyzed.
- Third, through the calculation of the lake (E/I) ratio, the supply relationship between groundwater and lake water and the development of the lake are analyzed.

INTRODUCTION

As the 'Third Pole' of the earth, the Qinghai–Tibet Plateau (QTP) is mainly underlain by high-altitude permafrost (Ran *et al.* 2018). Thermokarst lakes are common landscape features in the QTP, and they developed as a result of the thawing of ice-rich permafrost or melting of massive ground ice (Brown & Grave 1979; Hinzman *et al.* 1997). Climate change has a significant impact on water resources and the eco-environment in cold and arid regions of China (Wang *et al.* 1996; Toniolo *et al.* 2009). As a result, the occurrence of active thermokarst lakes may indicate that permafrost is warming and unstable (Zhou *et al.* 1996; Serreze & Walsh 2000). The thermokarst is mainly experienced in four stages of development, which include formation, expansion, stopping of expansion, water body drainage, and formation of another permafrost (Niu *et al.* 2008). The size, depth of the lake, and water temperatures are important factors determining the permafrost configuration around and beneath them (Lin *et al.* 2011). The mean annual temperature at the lake bottom may influence the configuration of the permafrost and talik further (Burn 2005).

Under the impact of warming climate and increasing precipitation, lake areas in the interior of the QTP have been increasing over the past few decades (Zhang *et al.* 2017). The number of thermokarst lakes in the Beiluhe River basin of the QTP has

increased approximately by 534, amounting to an augment in an area of 410 ha during the past four decades (Luo *et al.* 2015). The expansion of these lakes has fatally led to a series of environmental issues, such as changes in soil, ecology hydrology, and caused instability of important basic projects such as the Qinghai–Tibet highway and railway in the basin. In addition, thermokarst lakes threaten the stability of the ecosystem and hinder the sustainable development of the social economy (Gao *et al.* 2017a, 2017b).

The hydrogeochemical characteristic of the thermal melting lakes will change inevitably along with a series of material and energy exchanges in the thaw–freeze process. From the study on the hydrogeochemical genesis of some saltwater lakes, such as Qinghai Lake and Qarhan Salt Lake, showing the hydrogeochemical characteristics of typical salt lakes are mainly affected by the supply source and the evaporation (Sun *et al.* 1991; Zhang 2009; Zhang *et al.* 2010; Gou 2011). Numerous new thermokarst lakes were formed because of the disturbance of natural conditions after the construction of the Qinghai–Tibet railway (Li *et al.* 2020). The hydrogeochemical composition of lakes along the railway in the Beiluhe region was found to be lower than that of other regions which may be related to the formation conditions of lakes (Yang *et al.* 2016).

Stable isotope geochemistry plays a critical role in monitoring climate change (Li *et al.* 2012, 2013). As the common stable isotope, δD and $\delta^{18}O$ have a wide range of applications in evaluating the source and recharging of surface water. It can also indicate the interaction between surface water, groundwater, and rainfall in different regions. The values of ion concentrations of δD and $\delta^{18}O$ were proven to be useful tools for studying the hydrological processes of lakes on the Tibetan Plateau (Yang *et al.* 2016; Gao *et al.* 2017a, 2017b). Furthermore, Yang *et al.* (2016) demonstrated that thermokarst lake water was contributed 61.3% of the melting of ice-rich permafrost by using the isotopic method.

The active layer is the layer above the permafrost that freezes in the cold season and melts in the warm season (Zhang *et al.* 2015). It is the interface between the permafrost and the atmosphere for heat exchange. The seasonal freezing–thawing process of the active layer has an important impact on surface energy balance, water migration, and groundwater runoff (Anisimov *et al.* 1997; Hollesen *et al.* 2011). Based on the observation data, the melting of the active layers in the Wudaoliang area first began in late April, achieved the maximum depth in September melt, and quickly completed all the freezing processes in late October (Hu 2020).

In this study, the regimes of hydrogeochemical composition, δD and $\delta^{18}O$, in lakes and groundwater during the freezing–thawing process in the active layer were analyzed by using hydrogeochemical theory and mathematical statistics. The objectives of this paper are: (i) to determine the hydrogeochemical components of lake water in different freezing–thawing processes; (ii) to analyze the possible hydrogeochemical reactions in lake water; and (iii) to determine the recharge relationship between lake water and atmospheric precipitation and underground meltwater.

MATERIALS AND METHODS

Study area

The Beiluhe basin, a main part of the Hoh Xil Nature Reserve Region, lies in the interior of the QTP (Lin *et al.* 2011). This primary area of QTP experiences permafrost basin is 350 km away from Golmud City with an altitude of 4,600 m (Figure 1).

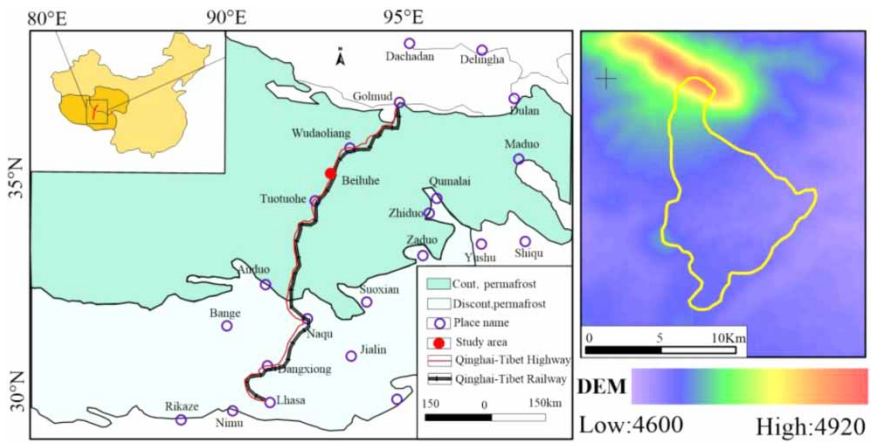

Figure 1 | Location of the study area in the QTP. Permafrost underlies 75% of the total area of the plateau and is relatively warm and in places, ice-rich. The study site is within the continuous permafrost zone.

The Beiluhe basin is located in an extremely continental climate zone and high solar radiation. The data recorded from 2005 to 2014 indicated that the mean annual air temperature is about −3.4 °C, while the precipitation is about 369.8 mm yr^{-1} (Yin *et al.* 2017). Over 90% of precipitation falls between May and September. The mean annual potential evaporation is about 1,317 mm yr^{-1}, much higher than the precipitation (Yin *et al.* 2017). Meanwhile, the annual variation of air temperature in the study area (+0.027 °C/annum) over the past 60 years has shown increasing trends, similar to that of precipitation processes (+154 mm/annum) (Gao *et al.* 2017a, 2017b). Permafrost is widely distributed in the study area because the multi-year ground temperature is −1.8 to −0.5 °C (Huang *et al.* 2011). The active layer thickness is 1.8–3.0 m, and the permafrost is generally 20–80 m thick; the geothermal gradient is 1.5–4.0 °C/100 m (Huang *et al.* 2011).

The regional strata consisted predominantly of lacustrine deposits of the upper Tertiary and diluvium of the Quaternary Holocene Series (silty clay). The ground surface, which is generally sparse in vegetation, is covered by fine sand with gravel (0.5–2.1 m in thickness), while the underlying layers include silty clay (up to 8 m in thickness in some places) and mudstone with sandstone interlayer (Lin *et al.* 2011).

Thermokarst lakes are widely distributed in the study area. The mean lake area in the region is 8,500 m^2, the largest lake is greater than 60,000 m^2, and the smallest one is less than 1,200 m^2 (Lin *et al.* 2011). The permafrost thickness ranges from 20 to 80 m, with an active layer of 1.8 to 3.0 m in thickness (Lin *et al.* 2011). The lakes in the study area are relatively small compared with those in the Kunlun mountainous region, Chumaerhe High Plain, and Beiluhe basin, whereas they are much deeper. Almost all the lakes in the study area have a depth of >1 m, and one of them is almost 3 m deep. The thermokarst lakes developed in the low-lying ground where ice-rich permafrost or massive ground ice exists.

Sample collection

The water samples of the Beiluhe River were collected in June, July, August, and October in 2019, and the sampling locations are shown in Figure 2. The freezing–thawing stages of the active layer that corresponds to the time of the four samples include the early thawing, middle thawing, late thawing, and freezing periods of the active layer.

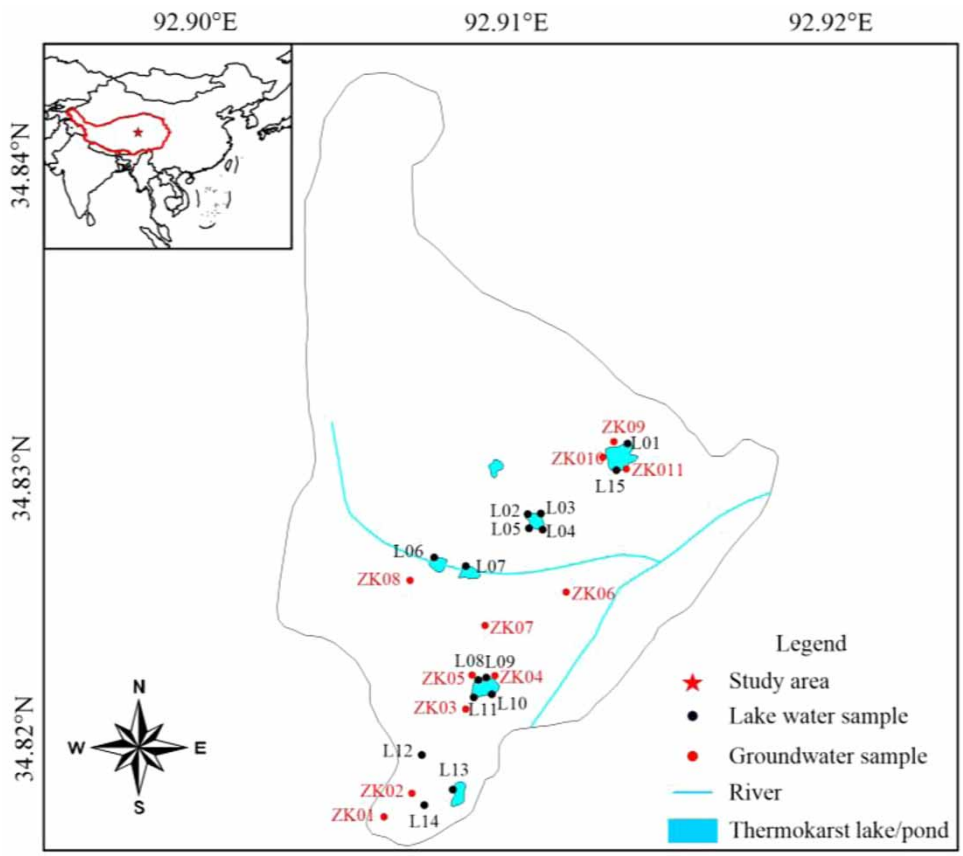

Figure 2 | Location of the study area.

There are over 15 lake samples and nine groundwater samples were collected, while part of the water sample may be missing because of the high degree of difficulty of sampling in some sampling sites. The water samples were sealed in PVC bottles and then taken back to the room for testing. Three bottles of water samples were collected at each sampling point. Two bottles of 500-ml water samples were used for general hydrogeochemical analysis and detection, while one bottle of 50-ml water sample was used for isotope detection.

Laboratory analysis and calculating method

Laboratory analysis

The temperature and pH of the samples can be measured directly by a portable water quality analyzer (6,250 °C) at the water sampling site. The contents of SO_4^{2-}, HCO_3^-, CO_3^{2-}, NH_4^+, and Cl^- in the lake water sample were determined by using the conventional titration method. Na^+ and K^+ were determined by flame color reaction and flame atomic absorption spectrometry (TAS990). EDTA titrimetric methods were adopted for analyzing Ca^{2+} and Mg^{2+}. The total dissolved solids are obtained by steaming the water sample dry and measuring its weight. F^- was determined by the ion-selective electrode (ICS-90A), and NO_2^- and NO_3^- were measured mainly by ion chromatography (precision ion meter).

The detection of hydrogen and oxygen stable isotopes were carried out by the Hebei University of Geosciences, which mainly measured the 1,000 deviation value of hydrogen and oxygen stable isotopes in lake water, underground water, and rainwater samples. The measurement is mainly performed by the newest L214-i instrument in the United States, and the accuracy of δD and $\delta^{18}O$ can reach 0.5 and 0.1‰.

Calculating method of dissolution/precipitation

The saturation of minerals, such as compounds ($MgCa(CO_3)_2$), calcite ($CaCO_3$), anhydrite ($CaSO_4$), and salt rock (NaCl), in lake water was calculated. To analyze the possible chemical reactions in the lake, the saturation index (SI) is defined as follows (Li *et al.* 2014):

$$\mathrm{SI} = \lg \frac{\mathrm{IAP}}{\mathrm{K}} \tag{1}$$

where IAP is the activity product of reactive mineral ions in water. K is the equilibrium constant of the mineral dissolution reaction. $SI > 0$, which indicates that the mineral is in a supersaturated state; $SI = 0$, which indicates that the minerals in the water are in a dissolved equilibrium state; and $SI < 0$ means that the mineral is not saturated.

Calculating the method of isotopic change during the freezing–thawing process

In this paper, the isotopic 1,000 deviation value is used to represent the isotopic content, which refers to the 1,000 deviation between the isotope ratio of the sample (*R* sample) and the standard sample isotope ratio (*R* standard),

$$\delta(‰) = \frac{R_{sample} - R_{standard}}{R_{standard}} \times 1,000 \tag{2}$$

The isotopic thousandth deviation (δ) is a dimensionless value that clearly reflects the size and trend of an isotope content in a sample

Calculating the method of evaporation-to-inflow estimation of lakes at different stages

The evaporation-to-inflow (E/I) of lakes is estimated at different stages for a particular lake in the study area. The amount of water that flows into the lake and the amount of water lost by the lake should be balanced dynamically within a certain period. However, it is difficult to calculate the lake water balance by using traditional hydrology methods due to the high altitude in the study area. Therefore, many scholars have adopted the E/I ratio of the lake as an important index to evaluate the balance process of lake water.

The E/I of the lake can be calculated by the mass balance method of stable isotopes. The calculation formula is expressed as follows:

$$\frac{E}{I} = \frac{\delta_I - \delta_L}{\delta_E - \delta_L} \tag{3}$$

In Equation (3), δ_L is the composition of hydrogen and oxygen isotopes in the lake; δ_I is the 1,000th deviation value of hydrogen and oxygen isotopes in groundwater flowing into the lake water and frozen soil, which is generally equal to the intersection point of the precipitation line in the region and the evaporation process line of the lake. Therefore, to calculate the E/I of the lake, the values of δ_I and δ_E need to be determined.

δ_E is the liquid-gas equilibrium fractionation factor (α) function, according to Horita & Wesolowski (1994), the empirical formula to calculate is expressed as follows:

$$^{18}O: \alpha = \exp\left(-7.685 \times 10^{-3} + \frac{6.7123}{T} - \frac{1.6664 \times 10^{3}}{T^{2}} + \frac{3.5041 \times 10^{5}}{T^{3}}\right) \tag{4}$$

$$D: \alpha = \exp\left(1158.8 \times T^{3} \times 10^{-12} - \frac{1620.1 \times T^{2}}{10^{6}} - 161.04 \times 10^{-3} + \frac{2.992 \times 10^{6}}{T^{3}}\right) \tag{5}$$

where T is the absolute temperature in units of K. Liquid water and gaseous water balance between fractionation factors (ε^*) is presented as follows:

$$\varepsilon^* = \alpha - 1 \tag{6}$$

where α is the isotope content of free air above the lake, and it can be estimated by using the following formula:

$$\delta_A = \frac{\delta_P - \varepsilon^*}{\alpha} \tag{7}$$

where δ_P is the 1,000th of the isotopic deviation value of atmospheric precipitation.

Dynamic fractionation coefficient ε_K is a function of air relative humidity h_s,

$$\varepsilon_K = C_K(1 - h_s) \tag{8}$$

The value of h_s is between 0 and 1, and C_K is the relevant parameter used to calculate the dynamic fractionation coefficient. The C_K of ^{18}O is 14.2‰, whereas that of D is 12.5‰ (Gonfiantini 1986).

Under the condition of continuous enrichment of isotopes, the stable isotopes in the lake will reach extreme value, and the calculation formula is presented as follows:

$$\delta^* = \frac{h_s\delta_A + \varepsilon_K + \frac{\varepsilon^*}{\alpha}}{h_s - 10^{-3} - 10^{-3}\frac{\varepsilon*}{\alpha}} \tag{9}$$

Gonfiantini (1986) studied isotopic equilibrium in lakes and obtained the following formula for calculating δ_E:

$$\delta_E = \frac{(\delta_L - \varepsilon^*)/\alpha - h_s\delta_A - \varepsilon_K}{1 - h_s + 10^{-3}\varepsilon_K} \tag{10}$$

Therefore, the values of relative humidity h_s, temperature T, and hydrogen and oxygen isotopes δD and $\delta^{18}O$ should be determined and substituted in atmospheric precipitation during the melting and freezing of the active layer. So, the E/I of the lake at different stages can be calculated. Temperature and h_s are available from the National Meteorological Data Network.

RESULT

Ion content of lake water

Simple statistics were carried out on the test results of lake water samples in the freezing–thawing process of the active layer (Table 1). Table 1 shows that the content distribution of each ion in different lakes varies to some extent. Meanwhile, most of the variation coefficient between 10 and 100% shows that the ions in the lakes are not evenly distributed in the region.

The content of each ion in the water sample in the study area was plotted as a boxplot (Figure 3). The contents of anions Cl^- and HCO_3^- and the cation such as $Na^+ - K^+$ in lake water are at a high level at different freezing–thawing stages in the active layer. The distribution of Ca^{2+}, Mg^{2+}, HCO_3^-, and SO_4^{2-} is relatively uniform, whereas the extreme values of Na^+ and Cl^- concentrations vary greatly with significant regional differences from the perspective of regional characteristics.

Moreover, the average concentrations of CO_3^{2-}, HCO_3^-, and Cl^- in the lake changed greatly in the freezing–thawing process of the active layer. During the melting process of the active layer to refreezing, pH concentration showed an increasing trend from 8.4 to 9.11 under the influence of aquatic plants' photosynthesis. The CO_3^{2-} concentration also increased gradually from 10.11 mg/L at the initial melting stage of the active layer to 49.29 mg/L, while the HCO_3^- concentration decreased to 156.43 from 249.00 mg/L. Obviously, the decreased range of HCO_3^- concentration is greater than the increased range of CO_3^{2-} concentration, which may be due to the conversion of part of HCO_3^- to other forms of carbon in the lake.

Types of lake water

In this study, Shukalev classification was employed to clarify the water types of thermokarst lakes. The classification results show that the hydrogeochemical types of lake water have certain regional differences (Figure 4).

Na^+, Ca^{2+}, and Mg^{2+}, which are located in Zones B and D, are predominant among cations. The anions, including HCO_3^- and Cl^-, are mainly located in the E and G regions. Besides, the sample in October is all distributed with the right of the sample points except for the lakes in the central region. The results obtained by the Piper graph indicated that the hydrogeochemical types of lakes in the study area were mainly mixed water samples of HCO_3·Cl – Na·Ca·Mg and Cl – Na·Mg.

Table 1 | Statistical table of lake water samples at different stages

	Project	T	pH	TDS	Na^+	Ca^{2+}	Mg^{2+}	CO_3^{2-}	HCO_3^-	Cl^-	SO_4^{2-}
Jun.	Mean	3.88	8.40	645.43	145.86	34.52	45.21	10.11	249.00	245.54	29.49
	Maximum	5.59	9.18	1,080.00	261.00	64.10	71.70	30.00	421.00	443.00	57.60
	Minimum	−4.16	7.79	256.00	34.60	24.00	14.60	0.10	171.00	42.50	14.40
	Standard	3.87	0.55	324.05	91.96	10.27	21.91	12.04	62.63	167.43	12.15
	Variable coefficient	24.4	6.56	50.21	63.05	29.74	48.46	119.04	25.15	68.19	41.21
Jul.	Mean	7.52	8.86	581.07	120.41	30.08	40.82	28.40	190.80	211.07	24.64
	Maximum	7.96	9.21	952.00	223.00	48.10	75.30	42.00	238.00	425.00	48.00
	Minimum	6.40	8.45	240.00	32.00	8.02	15.80	12.00	128.00	38.00	4.80
	Standard	0.68	0.25	287.14	75.52	9.00	19.42	10.84	29.25	154.12	14.11
	Variable coefficient	9.05	2.82	49.40	62.72	29.92	47.57	38.17	15.33	73.02	57.26
Aug.	Mean	7.13	9.01	598.57	130.65	28.44	41.99	42.43	160.76	223.64	22.56
	Maximum	9.53	9.71	960.00	240.00	104.00	65.60	72.00	421.00	415.00	43.20
	Minimum	5.43	7.90	220.00	23.40	12.00	15.80	0.10	61.00	28.00	3.84
	Standard	1.58	0.55	290.55	81.35	22.52	18.70	26.88	88.43	151.59	14.42
	Variable coefficient	22.18	6.07	48.54	62.26	79.19	44.54	63.35	55.01	67.78	63.92
Oct.	Mean	−2.62	9.11	605.43	129.26	30.34	43.74	49.29	156.43	230.86	25.37
	Maximum	−1.49	9.98	856.00	224.00	56.10	66.80	90.00	281.00	390.00	67.20
	Minimum	−5.10	7.81	284.00	27.20	14.00	17.00	0.10	48.80	34.00	4.80
	Standard	1.47	0.68	241.91	72.96	12.22	18.20	30.10	76.80	144.97	17.72
	Variable coefficient	56.23	7.41	39.96	56.45	40.28	41.60	61.07	49.09	62.80	69.84

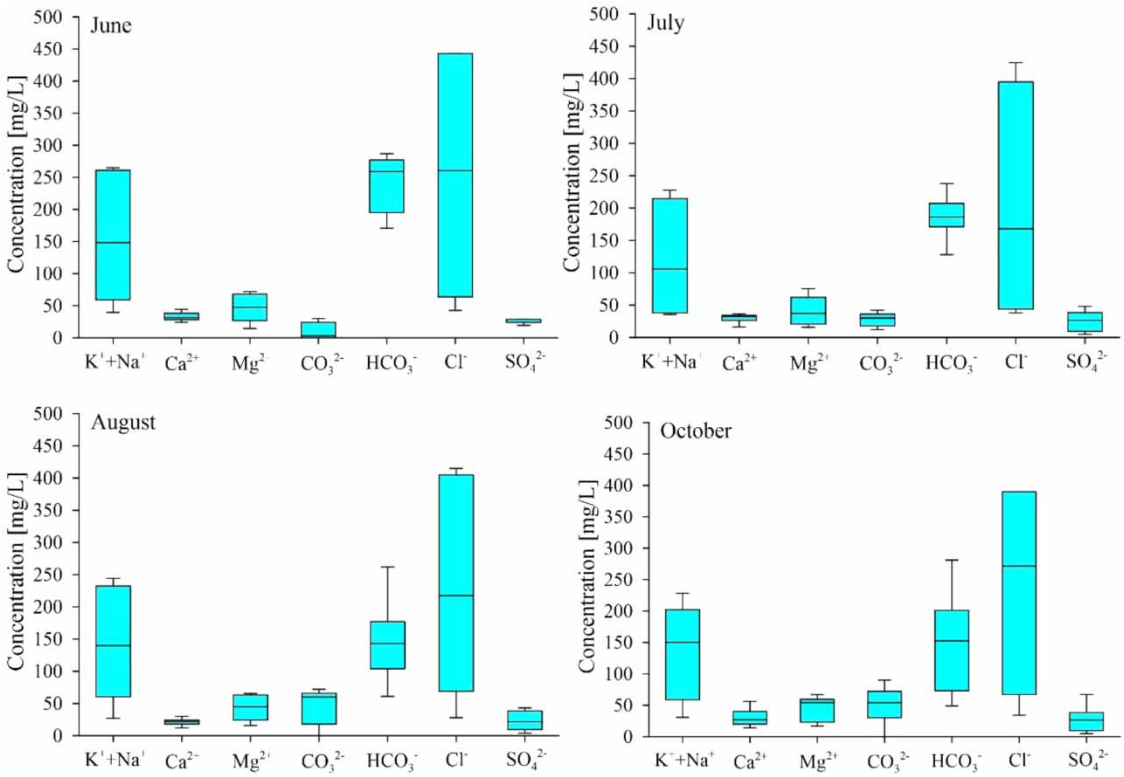

Figure 3 | Boxplot of main ion concentrations in lake water at different stages.

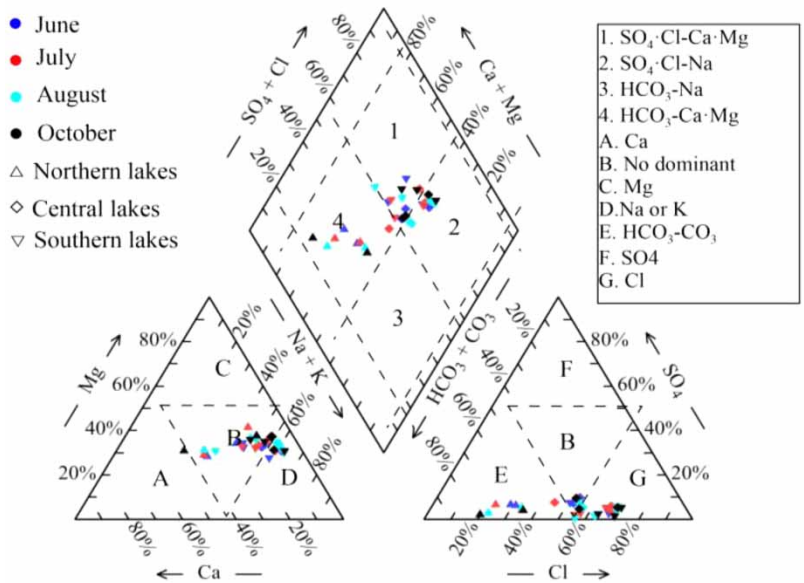

Figure 4 | Piper trigram of typical lakes.

Sources of lake water chemical components

Gibbs graphical method

The Gibbs graphs indicate that the source of the hydrogeochemical composition of surface water is mainly affected by rock weathering, evaporation and concentration, and meteoric precipitation. The Gibbs diagram of the lake is shown in Figure 5 during the melting of the active layer to the freezing process.

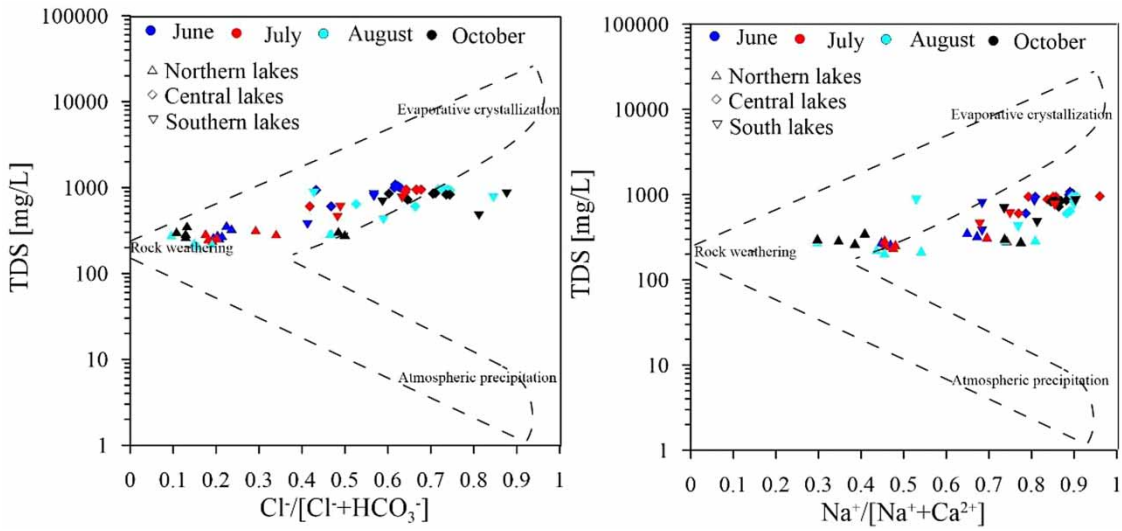

Figure 5 | Chemical Gibbs of lake water during the process of active layer melting to freezing.

Figure 5 shows that $Na^+/(Na^+ + Ca^{2+})$ in the lake is between 0.3 and 0.9, while $Cl^-/(Cl^- + HCO_3^-)$ is between 0.1 and 0.9. Lake water sample points are mostly distributed in the middle and upper parts of the Gibbs chart, which is controlled by evaporation and rock weathering. The hydrogeochemical compositions of the lakes in the north, central, and south of the study area were significantly different from one another. The hydrogeochemical compositions of the lakes in the north of the study area were significantly affected by rock weathering, whereas those in the central and south were mainly affected by evaporation and concentration.

Furthermore, the water chemistry of each lake in the Gibbs diagram shows a trend of migrating to the right during the thawing–freezing process of the active layer. This phenomenon indicates that the concentration of ions in the unfrozen water is increased by the freezing desalination of the active layer in the thawing–freezing process of the active layer, which has an important effect on the hydrogeochemical composition of the lake.

Ion proportional coefficient method

Through analyzing the ratio of ion normality, we can study the formation process of hydrochemical characteristics; otherwise, the characteristics of water quality on regional and temporal scales can be reflected. Eight thermokarst lakes in the study area were selected as the research objects to investigate the changes in the relevant ion proportionality coefficients on the time and regional scales (Figure 6).

Concentration coefficient of γNa/γCl. The magnitude of γNa/γCl can determine the sources of Cl^- and Na^+ and the level of salinity in lakes. Figure 6(a) shows that γNa/γCl in the northern lakes was greater than 1, whereas in most of the central and southern lakes was less than 1. Such a result was consistent with the TDS content in the lakes. The coefficient of γNa/γCl in the northern and central lakes fluctuated greatly on a time scale which indicates the freezing and thawing process had an influence on γNa/γCl. The γNa/γCl coefficient of the lakes in the southern part of the study area fluctuated less, which may be related to the hydrogeochemistry of the active layer.

Concentration coefficient of γHCO₃/γCa. The magnitude of $\gamma HCO_3/\gamma Ca$ is often used to analyze the sources of Ca^{2+} and HCO_3^- in water. Figure 6(b) shows that magnitude of $\gamma HCO_3/\gamma Ca$ in most lakes was between 1.5 and 3 at the initial melting time of the active layer, which may be caused by the dissolution of calcite. The magnitude of $\gamma HCO_3/\gamma Ca$ showed a slow decline over time, which may be mainly caused by the change in HCO_3^- concentration. As the active layer began to melt, the photosynthesis of aquatic organisms at the bottom continued to increase which eventually leads to the reduction of HCO_3^-.

Concentration coefficient of γCa/γMg. In Figure 6(c), the γCa/γMg coefficients of all lakes except lake H07 were less than 1 and gradually showed a decreasing trend in the different stages from the active layer melting to freezing. This phenomenon

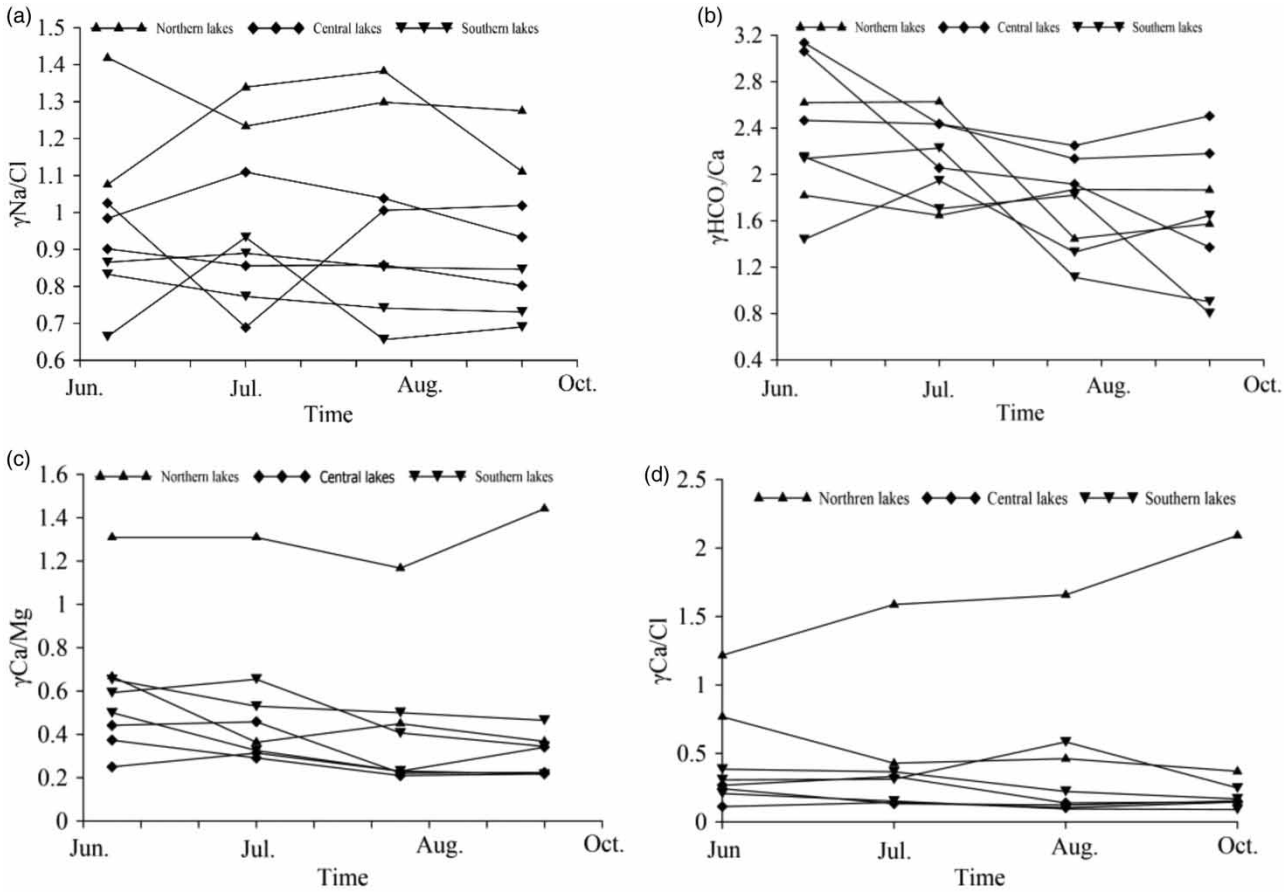

Figure 6 | Main ionic proportional coefficients in the lake water at different stages.

may be related to the decrease in Ca^{2+} concentration with the increase of CO_3^{2-} concentration in the lake. However, due to the time of H07 lakes formed earlier, resulting in the activities of the lake bottom layer is completely melt wear, this may lead to the gamma coefficient of Ca/Mg in gamma anomalies.

Concentration coefficient of γCa/γCl. The γCa/γCl coefficient is used to describe the dynamic characteristics of lake water. The lower the coefficient of γCa/γCl, the worse the water flow alternations in the lakes. When the coefficient of γCa/γCl is small, the water will flow slowly. In Figure 6(d), the γCa/γCl coefficients of all lakes water except the northern lake L07 at different stages were less than 1 and basically did not change with time, indicating that the alternative effect between lake water and groundwater flow was poor. The reason for the difference in L07 lake may be that the active layer at the bottom of the lake is melted through, which leads to the enhanced exchange between lake water and groundwater. Moreover, the γCa/γCl coefficient of L07 increased with time, which may be caused by the hydraulic connection enhanced between lake water and groundwater due to the warmer temperatures.

Hydrogeochemical process of lakes

Dissolution/precipitation

The SI can use to analyze chemical reactions that may occur in the lake. As shown in Figure 7, the SI of the calcite and dolomite in the lake water are all greater than 0 and will continuously increase in freezing–thawing stages, indicating that the dissolution reaction of minerals occurs in the lake water.

The SI of the salt rock and gypsum rock are less than 0, which indicates these two rocks do not exist at the bottom of the lake. The SI of gypsum rock in some lakes is getting lower on the time scale due to the reduction in Ca^{2+} concentration. Overall, the SI of salt rock does not change significantly with time.

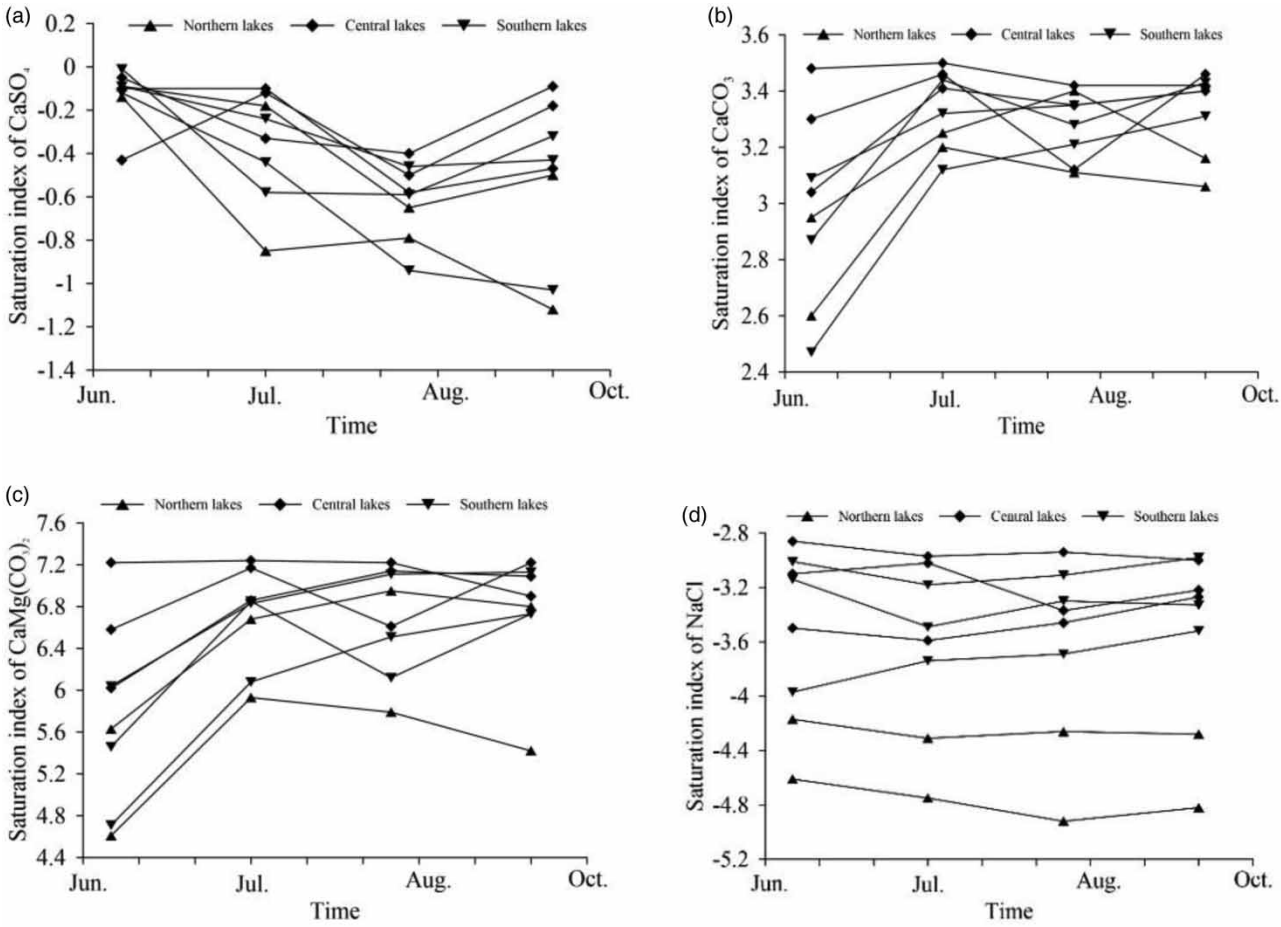

Figure 7 | SI of main minerals in lake water.

Cation alternate adsorption

The alternation of cation adsorption in lake water mainly occurs on the surface of lake bottom minerals. Some of the cations in lake water will be adsorbed on the soil particles to replace the originally adsorbed ions. Conventional ion adsorption ability from strong to weak is: $H^+ > Fe^{3+} > Al^{3+} > Ca^{2+} > Mg^{2+} > K^+ > Na^+$. The positive and negative relationship between $\gamma(Na^+ - Cl^-)$ and $\gamma(SO_4^{2-} + HCO_3^- - Mg^{2+} - Ca^{2+})$ is usually used to evaluate whether cationic alternate adsorption occurred in lake water (Figure 8). Only both of them are greater than 0 and Na^+ and Ca^{2+} have cation alternate adsorption.

As shown in Figure 8, $Na^+ - Cl^-$ and $(SO_4^{2-} + HCO_3^- - Mg^{2+} - Ca^{2+})$ in the northern lakes are all greater than 0 during the melting and freezing of the active layer, which indicates that cationic alternate adsorption may exist in the northern lakes. From the perspective of time, cationic alternate adsorption occurred in the L07 and L08 lakes at the initial melting stage of the active layer, whereas it only occurred in the L08 lake in the middle melting stage to the freezing stage. The cationic alternation adsorption in the L08 lake was the Na^+ replaced by Ca^{2+} due to the concentration of Na^+ in the northern lakes being higher than that of Ca^{2+}.

Reasons for changes in lake water chemical composition

Generally, lake water hydrogeochemical characteristics are mainly influenced by aquatic plants, groundwater runoff, temperature, and other conditions. Lake L06, which is located in the middle of the study area, is chosen as the representative lake to analyze the reasons for the changes in the hydrogeochemical characteristics of the lake water during the melting–freezing process of the active layer. The changes in the ion concentration in Lake L06 are shown in Figure 9.

The concentrations of CO_3^{2-}, HCO_3^-, and Cl^- and pH in Lake L06 showed significant differences during the melting–freezing process of the active layer, whereas SO_4^{2-}, Na^+, Ca^{2+}, and Mg^{2+} showed rarely differences over time. The reasons for the changes in the concentration of major ions in Lake L06 were analyzed.

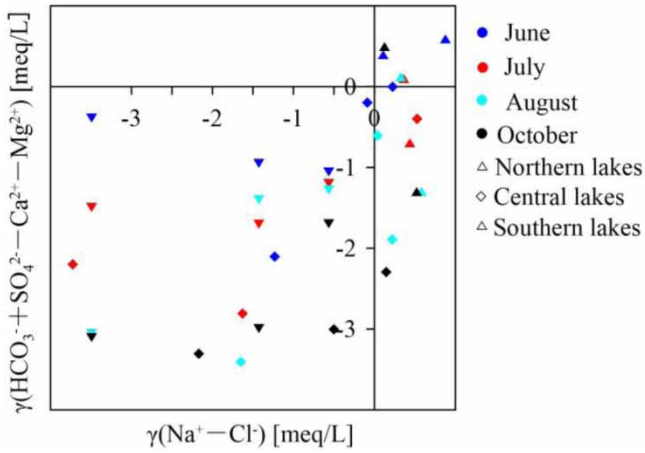

Figure 8 | $\gamma(Na^+ - Cl^-)$ and $\gamma(SO_4^{2-} + HCO_3^- - Mg^{2+} - Ca^{2+})$.

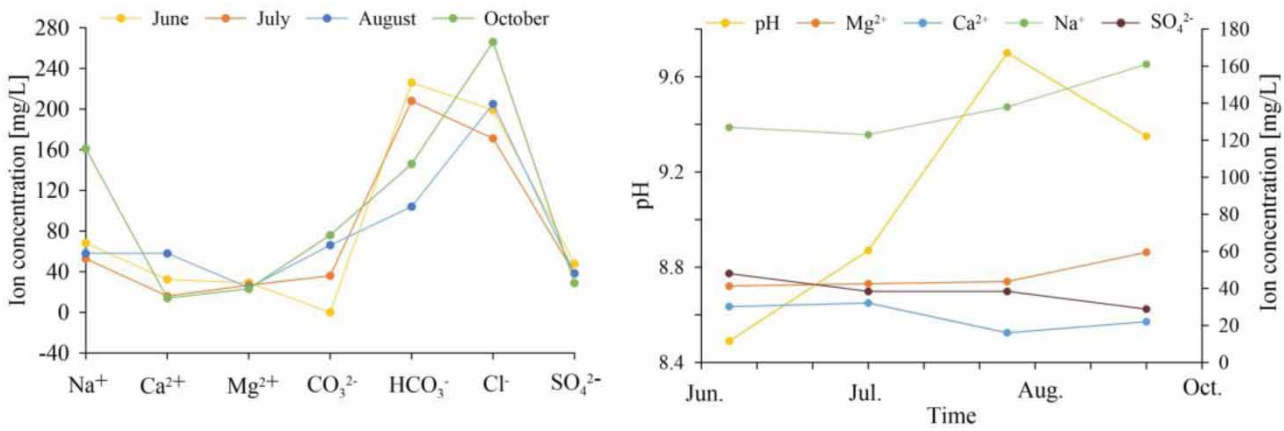

Figure 9 | Changes of main ions in L06 lake over time.

In the early stage of the melting of the active layer, the lake surface had almost melted. At this stage, the surface water thawed the top of the active layer, whereas the bottom of the active layer was mostly frozen.

In the middle of the active layer melting, the average daily temperature reached the maximum. The warming of the lake water increased the melting rate of the active layer. Compared with the initial melting stage of the active layer, the differences in the hydrogeochemical composition in the lake were reflected in the increase in CO_3^{2-} concentration and pH, and the decrease in HCO_3^- and Cl^- concentrations. In this stage, aquatic organisms were more active in photosynthesis. Part of the CO_2 required for photosynthesis is produced by the hydrolysis of HCO_3^-, the other part obtained through the CO_2 in lake water coming from the atmosphere. Naturally occurring process in the water involves the CO_2 dissolution as Equation (11) and the inorganic carbon dissociation reactions as Equation (12):

$$CO_2 + H_2O \leftrightarrows H_2CO_3 \tag{11}$$

$$H_2CO_3 + OH^- \leftrightarrows HCO_3^- + H_2O \tag{12}$$

$$H_2CO_3 \rightarrow HCO_3^- + H^+ \tag{13}$$

$$HCO_3^- \rightarrow CO_3^{2-} + H^+ \tag{14}$$

Due to the continuous consumption of CO_2 in the lake by photosynthesis, Equations (11) and (12) both moved to the left continuously. Then this leads to the reduction of HCO_3^- concentration, whereas the increase of OH^- concentration in the lake. According to the carbonic acid equilibrium, the increase in pH must convert part of HCO_3^- into CO_3^{2-} as shown in Equation (14). From the point of the conservation of carbon mass in lake water, the reduction of HCO_3^- concentration in

the lake water was less than the rise of CO_3^{2-} concentration. Part of the CO_2 consumed by aquatic plants in photosynthesis must come from the CO_2 dissolved in lake water. The decrease of Cl^- content in lake water may be caused by precipitation or permafrost meltwater. Precipitation or permafrost meltwater with relatively low ion concentration entered into lake water, thereby resulting in a certain decrease in Cl^- content in lake water.

In the later period of the melting of the active layer, the melting speed of the active layer reached the maximum. Compared with the initial melting stage of the active layer, the contents of pH, Cl^-, CO_3^{2-}, and Na^+ in the lake increase, whereas the content of HCO_3^- continued to decrease. In this stage, the changes in HCO_3^-, CO_3^{2-}, and pH were mainly caused by the photosynthesis of aquatic organisms at the bottom of the lake. Although the effect of groundwater on the runoff of lake water enhanced and the groundwater with a high HCO_3^- content replenished into the lake water, the HCO_3^- in the lake water was not sufficient to balance the consumption of photosynthesis due to the strong photosynthesis of aquatic plants in the lake water. As a result, the HCO_3^- concentration in the lake water continued to decrease, while the CO_3^{2-} concentration and pH continued to increase. The slight increase in Cl^- and Na^+ contents may be due to the following reasons: First, the discharge of groundwater with high Cl^- and Na^+ concentrations into lake water had a certain effect on the Cl^- and Na^+ contents in lake water. Secondly, the evaporation of the active layer was strong in the later period of melting which may increase the contents of Cl^- and Na^+.

During the freezing period of the active layer, the temperature and the precipitation of the lake water decrease. The water began to freeze simultaneously from the surface and the top surface of the active layer to the center. Compared with the previous stage, the concentration changes of each ion in the lake were reflected by the increase in the concentrations of CO_3^{2-}, HCO_3^-, Na^+, and Mg^{2+}, whereas the decrease in the pH of the lake. From the thawing to the freezing stage of the active layer, the precipitation decreased significantly, and evaporation and crystallization played an obvious control role on the concentration of all ions in the lake. At the same time, the concentration of almost all ions increased under intense evaporation. The decrease in temperature increased the solubility of CO_2 in the lake and reduced the intensity of photosynthesis. The decrease in pH is affected by the carbonic acid equilibrium system. As the consumption of CO_2 decreases, the equilibrium in Equation (11) moved to the left and increased the HCO_3^- concentration.

Characteristics of isotopic change during the freezing–thawing process

Characteristics of hydrogen and oxygen isotope composition

Isotopes of lakes and groundwater in the study area were collected in June (early thawing period of active layer), July (middle thawing period of active layer), August (late thawing period of active layer), and October (freezing period of active layer). Among them, rainwater samples were collected in June and August, which was helpful to understand the relationship between lake water and groundwater in the study area.

Table 2 shows that during the melting to refreezing of the active layer, δD and $\delta^{18}O$ in the groundwater and the lake water were less than 0. Furthermore, δD and $\delta^{18}O$ in the groundwater were always less than the lake water, which indicated that the heavy isotope content in the former was higher than in the latter. In addition, the content of δD in the lake water and groundwater was lower than that of $\delta^{18}O$, which also indicated that the degree of fraction of heavy isotopes was lower than light isotopes.

E/I estimation of lakes at different stages

The E/I of lakes at different stages for a particular lake in the study area was estimated. The amount of water flowing into the lake and the amount lost by the lake should be in dynamic balance at set times. However, calculating the lake water balance

Table 2 | Statistical table of hydrogen and oxygen stable isotopes in lake water

	δD			$\delta^{18}O$		
Time	Mean	Min.	Max.	Mean	Min.	Max.
Jun.	−44.83	−64.11	−35.06	−5.83	−8.59	−4.22
Jul.	−33.02	−36.69	−26.50	−4.42	−5.21	−3.39
Aug.	−46.46	−83.93	−27.23	−5.93	−11.61	−3.09
Oct.	−49.00	−62.19	−37.02	−6.22	−8.36	−4.35

Table 3 | E/I statistics of lakes at different time periods

	Jun.		Jul.		Aug.		Oct.	
Lake	$\delta^{18}O$	δD	$\delta^{18}O$	δD	$\delta^{18}O$	δD	$\delta^{18}O$	δD
1	1.12	1.30	0.75	0.74	0.72	0.68	0.90	1.21
2	1.06	1.11	0.73	0.75	0.48	0.36	0.86	1.37
3	1.05	1.10	0.77	0.77	0.72	0.67	0.89	1.25
4	1.05	1.10	0.74	0.75	0.73	0.70	0.89	1.25
5	1.06	1.11	0.75	0.74	0.74	0.70	0.92	1.16
6	1.06	1.11	0.77	0.77	0.76	0.72	0.92	1.15
7	1.10	1.19	0.77	0.77	0.76	0.72	0.91	1.18
8	1.11	1.17	0.79	0.80	0.41	0.21	0.92	1.16

by using traditional hydrology methods was difficult due to the high altitude in the study area. Therefore, many scholars adopt the E/I ratio of the lake as an important index to evaluate the lake water balance process.

To facilitate the description of the calculation results, the eight lakes in the study area were named as 1–8 in the order from north to south. The calculation results of E/I at different stages were statistically analyzed (Table 3).

Table 3 shows that the E/I of the lakes in June, July, and August has rarely difference, whereas in October was large. The temperature dropped significantly in October, thereby enhancing the fractionation effect of isotopes. The atomic mass of hydrogen was much lighter than that of oxygen atoms, so the fractionation effect was significantly stronger than that of oxygen atoms, thereby resulting in some differences in the calculation results.

Furthermore, the value of E/I reached the maximum in the initial melting stage and the active layer freezing stage, whereas reached the minimum in the middle and late periods of the melting of the active layer.

With increasing evaporation in July and August, the precipitation and the depth of the melting of the active layer both reach the maximum which will increase recharge to the lake. Therefore, the E/I ratio of the lake is the minimum in July and August. On the contrary, the E/I is relatively large in June and October due to the weakly runoff effect of groundwater. The E/I characteristics of lakes at different stages verified the influence of freezing–thawing on groundwater runoff in the study area from the perspective of isotopes. Since the main drainage mode of the lake is evaporation, the evaporation of the lake in July and August is smaller than that of the groundwater, indicating that the lake is expanding when the active layer begins to melt until it is completely melted.

DISCUSSION

With the warming of the global climate, the expansion of hot melt lakes has become irreversible. It will lead to a series of environmental issues, including soil, ecology, and hydrology changes. The formation and development of lakes will release sodium from permafrost into the soil system, producing sodic or locally salinized soil, and subsequently degrading alpine vegetation.

Although the processes governing the formation and thawing of lake ice depend on multiple interacting meteorological and limnological factors (Gu & Stefan 1990), air temperature is considered to be the dominant factor. Toniolo *et al.* (2009) found that natural factors, which generally refer to the climatic environment, are major factors affecting the formation of hot melt lakes. The increase of temperature will lead to the increase of active-layer thickness, the melting of underground ice, and then the formation of hot melt lake in low terrain. Moreover, climate change directly causes lake temperatures, water levels, and the formation of water chemistry (Adrian *et al.* 2009).

In the form of global warming, it is a fact that the temperature of the QTP has generally increased. In this case, the rise of temperature will accelerate the development of hot karst lakes so that the number and area of hot karst lakes will change greatly. This paper studies the formation mechanism and evolution process of hot karst lakes under climate change conditions, which is helpful to grasp the water cycle process and future expansion direction of the lakes, and provides corresponding theoretical basis for harm reduction.

CONCLUSION

This paper clarified the water chemistry types of the hot melt lakes in the Wudaoliang area of Beiluhe and analyzed the reasons affecting the chemical composition of the water, and the E/I of different stages of hot melt.

1. The hydrogeochemical types of lakes showed regional differences. The northern lakes were mainly HCO_3·Cl – Na·Ca·Mg mixed water samples, whereas the central and southern lakes in the study area were Cl – Na·Mg evaporated water samples. And hydrogeochemical types of lakes are affected by evaporation and concentration and rock weathering.
2. The ion proportional coefficient at different stages reflects that the main ions in lake water may be related to the dissolution of salt rock, calcite, and dolomite. The SI of dolomite and calcite show that they control the components of hydrogeochemistry of lakes. The SI of salt rock and gypsum rocks indicate these two minerals are basically completely dissolved.
3. Atmospheric precipitation, evaporation, thawing of permafrost water, freezing desalination of the active layer, and the photosynthesis of aquatic plants are the main factors that cause the changes in pH, HCO_3^-, CO_3^{2-}, Ca^{2+}, Na^+, Cl^-, and Mg^{2+} concentrations in the lake.
4. With the influence of air temperature, E/I values show regular changes in different stages. The E/I of the lake and the recharge of groundwater to the lake both reach the maximum when the thickness of the unfrozen layer reaches the maximum in the middle and late stages of the melting of the active layer.

The melting and freezing of the active layer is a relatively complicated process, accompanied by the conversion of material energy. Although the four sampling times are in different stages, the four sampling times are relatively little. It is recommended to increase the number of samplings and to sample and analyze the water samples in the study area in different seasons to improve the existing conclusions.

ACKNOWLEDGEMENTS

We acknowledge the Beiluhe Scientific Research Station of CAS and the China University of Geosciences for their technical support during the experiment. This research was funded by the National Science Foundation of China, Grant No. 41730640 – Environmental and Hydrological Effects of the thermokarst Lakes in the Permafrost Region of the QTP – and the Fundamental Research Funds for the Central Universities, CHD, Grant No. 300102290401. This research was mainly supported by Cold and Arid Regions Environmental and Engineering Research Institute, Chinese Academy of Sciences. We are grateful to the anonymous reviewers for their helpful comments and constructive suggestions.

AUTHOR CONTRIBUTIONS

Y.F., W.W., and Z.L. designed the test and wrote the manuscript; H.H. and Q.L. analyzed the data, drew pictures, and checked the manuscript. All authors gave comments and contributed to the final version of the manuscript.

COMPETING INTEREST

The authors declare that they have no conflict of interest.

DATA AVAILABILITY STATEMENT

All relevant data are included in the paper or its Supplementary Information.

REFERENCES

Adrian, Rita, O'Reilly, Catherine M., Zagarese, Horacio, Baines, Stephen, B., Hessen, Dag, O., Keller, Wendel, Livingstone, David, M., Sommaruga, Ruben, Straile, Dietmar, Van Donk, Ellen, Weyhenmeyer, Gesa, A., Winder & Monika, 2009 Lakes as sentinels of climate change. *Limnology and Oceanography* **54**, 2283–2297.

Anisimov, O. A., Shiklomanov, N. I. & Nelson, F. E. 1997 Global warming and active-layer thickness: results from transient generalcirculation models. *Global and Planetary Change* **15** (3–4), 0–77.

Brown, J. & Grave, N. A. 1979 Physical and Thermal Disturbance and Protection of Permafrost. U.S. Army CRREL, Special Report, pp. 5–793.

Burn, C. R. 2005 Lake-bottom thermal regimes, western Arctic coast, Canada. *Permafrost and Periglacial Progresses* **6**, 355–367.

Gao, Z., Niu, F., Wang, Y., Luo, J. & Lin, Z. 2017a Impact of a thermokarst lake on the soil hydro logical properties in permafrost regions of the Qinghai-Tibet Plateau, China. *Science of the Total Environment* **574**, 751–759.

Gao, Z., Lin, Z., Niu, F., Luo, J., Liu, M. & Yin, G. 2017b Hydrochemistry and controlling mechanism of lakes in permafrost regions along the Qinghai-Tibet Engineering Corridor, China. *Geomorphology* **297**, 159–169.

Gonfiantini, R. 1986 Environmental isotopes in lake studies. *Handbook of Environmental Isotope Geochemistry* **2**, 113–168

Gou, Q. 2011 *The Research of China Chaerhan Salt Lake Resource Environmental Evolution*. Hunan Normal University. China.

Gu, R. & Stefan, H. G. 1990 Year-round temperature simulation of cold climate lakes. *Cold Regions Science and Technology* **18**, 147–160.

Hinzman, L. D., Goering, D. J., Li, S. & Kinney, T. C. 1997 Numeric simulation of thermokarst formation during disturbance. *Disturbance and Recovery in Arctic Lands: An Ecological Perspective*. Kluwer Academic Publishers, Dordrecht, The Netherlands, 621.

Hollesen, J., Elberling, B. & Jansson, P. E. 2011 Future active layer dynamics and carbon dioxide production from thawing permafrost layersin Northeast Greenland. *Global Change Biology* **17**, 911–926.

Horita, J. & Wesolowski, D. J. 1994 Liquid-vapor fractionation of oxygen and hydrogen isotopes of water from the freezing to the critical temperature. *Geochimica Et Cosmochimica Acta* **17**, 3425–3437.

Hu, H. 2020 *Heat and freezing and thawing conditions of qinghai-tibet plateau typical karst water geochemical process*. China, Chang'an University.

Huang, W. F., Li, Z. J., Niu, F. J. & Lin, Z. J. 2011 Structural features of thermokarst lake ice in Beiluhe Basin of Qinghai-Tibet Plateau. *Shuili Xuebao* **42** (11), 1277–1282.

Li, P., Wu, J. & Qian, H. 2012 Assessment of groundwater quality for irrigation purposes and identification of hydrogeochemical evolution mechanisms in Pengyang County, China. *Environmental Earth Sciences*, 2211–2225.

Li, P., Qian, H., Wu, J., Zhang, Y. & Zhang, H. 2013 Major ion chemistry of shallow groundwater in the Dongsheng Coalfield, OrdosBasin China. *Mine Water and the Environmen* **32**, 195–206.

Li, P., Wu, J. & Qian, H. 2014 Hydrogeochemistry and quality assessment of shallow groundwater in the southern part of the Yellow River alluvial plain (Zhongwei section) Northwest China. *Earth Sciences Research Journal* **18** (1), 27–38.

Li, J., Wang, W., Wang, D., Li, J. & Dong, J. 2020 Hydrogeochemical and stable isotope characteristics of lake water and groundwater in the Beiluhe Basin, Qinghai-Tibet Plateau. *Water* **12**, 2269.

Lin, Z., Niu, F., Liu, H. & Lu, J. 2011 Hydrothermal processes of Alpine Tundra Lakes, Beiluhe Basin, Qinghai-Tibet Plateau. *Cold Regions Science and Technology* **65**, 466–455.

Luo, J., Niu, F., Lin, Z., Liu, M. & Yin, G. 2015 Thermokarst lake changes between 1969 and 2010 in the Beilu River Basin, Qinghai -Tibet Plateau, China. *Journal of Science China Press* **60** (09), 871.

Niu, F. J., Xu, J., Lin, Z. J. & Wang, P. 2008 Engineering activity induced environmental hazards in permafrost regions of Qinghai-Tibet Plateau. In: *Proceedings, Ninth International Conference on Permafrost: Fairbanks*, Alaska, United States Permafrost Association, pp. 1287–1292.

Ran, Y., Li, X. & Cheng, G.-D. 2018 Climate warming over the past half century has led to thermal deg radiation of permafrost on the Qinghai -Tibet Plateau. *Cryosphere* **12**, 595–608.

Serreze, M. C. & Walsh, J. E. 2000 Observational evidence of recent change in the northern high-altitude environment. *Climate Change* **46**, 159.

Sun, D., Tang, Y., Xu, S. & Han, Z. 1991 Preliminary study on chemical evolution of lake water in Qinghai Lake. *Journal of Chinese Science Bulletin* **36**, 1172–1174.

Toniolo, H., Kodial, P., Hinzman, L. D. & Yoshikawa, K. 2009 Spatio-temporal evolution of a thermokarst in Interior Alaska. *Cold Regions Science and Technology* **56** (1), 39–49.

Wang, S., Zhao, X., Guo, D. & Huang, Y. 1996 Response of frozen ground to climatic change in the Qinhai-Xizang Plateau. *Journal of Glaciology & Geocryology* **18**, 157–165.

Yang, Y., Wu, Q., Yun, H., Jin, H. & Zhang, Z. 2016 Evaluation of the hydrological contributions of permafrost to the thermokarst lakes on the Qinghai -Tibet Plateau using stable isotopes. *Global and Planetary Change* **140**, 1–8.

Yin, G., Niu, F., Lin, Z., Luo, J. & Liu, M. 2017 Effects of local factors and climate on permafrost conditions and distribution in Beiluhe basin, Qinghai-Tibet Plateau, China. *Science of the Total Environment* **581-582**, 472–485.

Zhang, F. 2009 *Water Chemistry and Chemical Wrathering at Lake Qinghai and Lake Daihai Catch Ments*. Chain, Nanjing Agricultural University.

Zhang, K., Lan, J. H., Shen, Z. X. & Xu, H. 2010 The chemical composition and quality evaluation of surface water in Qinghai Lake areas. *Journal of Earth Environment* **1**, 162–168.

Zhang, G., Yao, T., Shum, C., Yi, S., Yang, K., Xie, H. & Feng, F. 2017 Lake volume and groundwater storage variations in Tibetan Plateau's endorheic basin. *Geophysical Research Letters* **44** (11), 5550–5560.

Zhang, M., Zhi, W. & Ke, X. 2015 Analysis on water and heat migration law of permafrost active layer in Beiluhe River. *Journal of Arid Land Resources and Environment* **29** (09), 176–181.

Zhou, Y., Wang, Y., Gao, X. & Yue, H. 1996 Ground temperature, frozen ground distribution and climate warming in Northeast China. *Journal of Glaciology and Geocryology* **18** (special issue), 139–147.

First received 12 September 2021; accepted in revised form 18 December 2021. Available online 28 January 2022